# 論文 / 著書情報
# Article / Book Information

| | |
|---|---|
| 論題(和文) | |
| Title(English) | High-Temperature Raman Spectroscopy of Na_2_O-RO-SiO_2_ Melts |
| 著者(和文) | 前原輝敬, 矢野哲司, 柴田 修一 |
| Authors(English) | Terutaka Maehara, Tetsuji Yano, Shuichi Shibata |
| 出典(和文) | , Vol. , No. , pp. O-10-022 |
| Citation(English) | XX International Congress on Glass, Kyoro, Japan, Vol. , No. , pp. O-10-022 |
| 発行日 / Pub. date | 2004, |

# High-temperature Raman spectroscopy of $Na_2O$-RO-$SiO_2$ melts

Terutaka Maehara*, Tetsuji Yano & Shuichi Shibata
*Department of Chemistry and Materials Science, Tokyo Institute of Technology,*
*S7-4, O-okayama 2-12-1, Meguro-ku, Tokyo 152-8550, Japan*
tmaehara@glass.ceram.titech.ac.jp

High-temperature Raman spectra of (33-$x$)$Na_2O$-x$RO$-67$SiO_2$ glass melts (R=Mg, Ca, Ba; $x$=0-25 in mol%) were measured at various temperatures from 1500ºC to room temperature. The equilibrium constants $K_R$ and the enthalpy change $\Delta H$ for the reaction $2Q^3 \Leftrightarrow Q^2 + Q^4$ in the melts were estimated by the band deconvolution of the spectra. In the melts of R=Mg and Ca, $\Delta H$ at $x \leq 17$ decreases gradually with increasing $x$, whereas, at $x>17$ it steeply decreases. On the other hand, in the melts of R=Ba, $\Delta H$ show a steady decrease with increasing $x$ even at $x>17$. These results suggest that the modifying cation governing the $Q^n$ equilibrium is surely switched from sodium to alkaline-earth ion with increasing $x$.

(Key words: melt structure, $Q^n$ equilibrium, soda-lime glass, $Na_2O$-RO-$SiO_2$ system, high-temperature Raman spectroscopy)

## 1. Introduction

$M_2O$-RO-$SiO_2$ glass is one of the most fundamental systems because most of the commercial glass products like sheet glass, container glass, CRT glass and optical glass have the compositions modifying this system. In the development of glass composition, types of alkali and alkaline-earth oxides, and their amounts have been adequately chosen to obtain the glasses with suitable properties for their application, i.e., chemical durability, electrical resistivity, strain point, workability and so on. These properties are affected by not only the ionic character of modifying cation but also the glass framework related to the configuration of modifying cations. Since most of glass products are obtained by the melt-quenching method, the structures from the melting temperature to the room temperature would be important to understand the resultant glass properties.

The framework of silicate glass consists of various types of $SiO_4$ tetrahedral units $Q^n$, where n is the number of bridging oxygen in tetrahedra. The molar fractions of individual $Q^n$ in silicate glass had been determined by $^{29}$Si MAS-NMR [1,2]. However, it is less informative in the melt at high temperature because the site-exchange frequency between different $Q^n$ becomes faster than Lamor frequency of nuclear spin [3,4]. Raman spectroscopy had also been used as an alternative method, by which we can know the relative amount of $Q^n$ units in the melt even at high temperature [5-10]. The $Q^n$ distribution in alkali silicate melts is known to change with both modifying cation type and temperature along with the following equilibrium reaction.

$$2Q^3 \Leftrightarrow Q^2 + Q^4 \quad (1)$$

However, the quantitative information of the structure of $M_2O$-RO-$SiO_2$ glasses and melts have not been clarified, and the effects of mixing of modifying oxides on the equilibrium reaction (1) have not been well understood.

Our group has shown that the employment of the pulse laser for the excitation source is beneficial to reduce the influence of the radiant light from high-temperature melts on the Raman scattering signals [11]. We applied it to alkali borate melts and alkali silicate melts, and succeeded in describing the melt structures and their relations with the glass and/or melt properties [12-14].

In the present paper, the high-temperature Raman spectra of (33-$x$)$Na_2O$-$x$RO-67$SiO_2$ glass melts (R=Mg, Ca, Ba; $x$=0, 8, 17, 25) were measured at various temperatures from 1500ºC to room temperature. The information of $Q^n$ structures of these glass-melts was estimated by the band deconvolution of the spectra. The effects of mixing of alkali and alkaline-earth oxides on the framework of melts are discussed based on the equilibrium reaction (1).

## 2. Experimental

### 2.1 Sample preparation

Glass samples with the compositions of (33-$x$)$Na_2O$-$x$RO-67$SiO_2$ (R=Mg, Ca, Ba; $x$=0, 8, 17, 25) were prepared by the conventional melting and quenching method. Reagent grade raw materials of $Na_2CO_3$, $MgCO_3$, $CaCO_3$, $BaCO_3$ and $SiO_2$ were mixed and melted in a platinum crucible for 2hours. Melting temperature was 1400-1600ºC depending on the glass composition. To ensure the glass homogeneity, the glasses were crushed and re-melted for 2hours. After the second melting, the glass melt was poured into the pre-heated graphite molds to obtain glass blocks and rod-shaped samples of 15mm in diameter. They were immediately transferred to an annealing furnace preheated to $T_g$+20ºC of the corresponding glasses. The glass samples were held at the annealing temperature for 1hour and then cooled to room temperature by 1ºC·min$^{-1}$. Samples were cut into final dimensions: blocks of 10x15x20 mm for polarized Raman scattering measurements, and a rods of 15x50mm for high-temperature Raman scattering measurements with polished end faces of optical grade.

### 2.2 Raman scattering measurements

Polarized Raman scattering measurements (HH and VH) at room temperature were carried out in 90º orientation using the measurement setup shown in Fig.1 (a). The polarized plane of the excitation laser was rotated using a half wave plate inserted in the laser beam line. The second harmonic of Q-switch Nd:YAG laser (532nm) was used as an excitation source. The pulses were of 5nsec duration time and 10Hz repetition rate. Raman scattering signal through a Gland-Thompson polarized prism, a notch filter and a 25cm-length double monochromator was detected by an image-intensified CCD array-type detector with the computer-controlled nsec-order electrical gate. The obtained spectra were corrected by using Bose-Einstein population factor.

Figure 1 (b) shows the setup for the high-temperature Raman scattering. The rod sample was placed in a platinum crucible with inner diameter of 15mm and the temperature was controlled within ±2ºC by a compact electric furnace. Second harmonic of Q-switch Nd:YAG laser (532nm) irradiated the sample, and Raman scattered light was collected in the back scattering geometry using a mirror and lenses. In 1500-800ºC range temperatures typical measurements were carried out by cooling step by step at an interval of 100ºC. On the other hand, below 700ºC, measurements were made by heating from room to high temperature at certain interval to avoid crystallization. In high-temperature Raman scattering, only HH polarized spectra were measured.

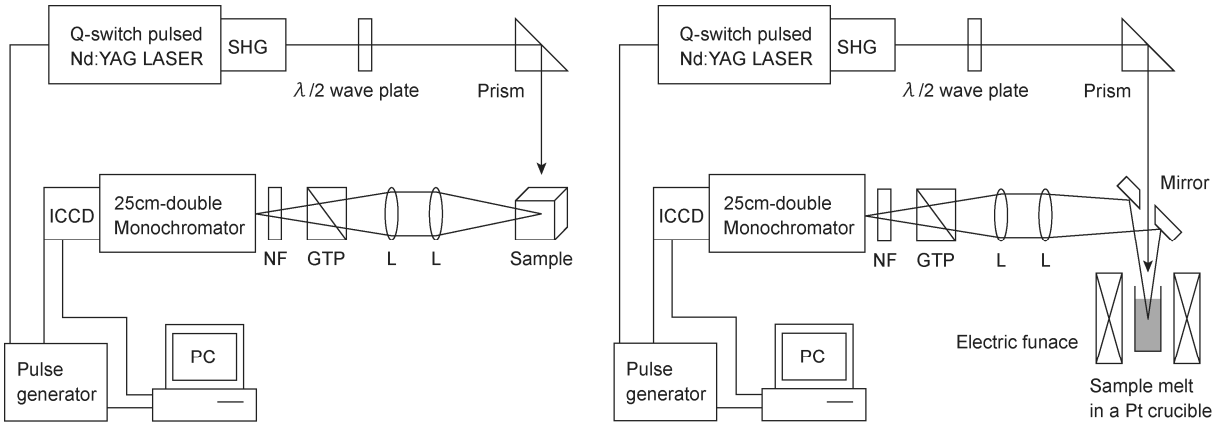


**(a) Polarizing Raman scattering measurement.** **(b) High-temperature Raman scattering measurement.**

Fig.1 Schematic illustration of the setup for measuring Raman scattering. A pulsed SHG-Nd:YAG laser (532nm) was used as an excitation source. Setup for (a) polarized and (b) high-temperature Raman scattering measurement. (GTP) Gland-Thompson polarizing prism, (NF) notch filter, (L) lens and (ICCD) Intensified CCD array-type detector.

### 2.3 Spectrum analysis

The reliable deconvolution of the bands is essential to obtain the information of $Q^n$ structures. In Raman spectra of silicate systems, the Si-$O^-$ stretching vibrations of $Q^2$ and $Q^3$ are located in the high-frequency region of 900 to 1200$cm^{-1}$. In order to define the deconvolution parameters; the number of components, the peak position and the FWHM (full width at half maximum), HH and VH spectra at the room temperature were simultaneously deconvoluted by Levenberg-Marquardt method [15]. The same peak positions and the FWHMs were used, while only about 5$cm^{-1}$ differences between HH and VH spectra were allowed because of spectral resolution limit of the monochromator. Deconvolutions of the high-temperature Raman spectra were also carried out taking into account the parameters at room temperature. In these band deconvolution procedures, Gaussian-shaped components were used to fit the original spectra.

The $Q^n$ distribution is derived from the intensity ratio of the band area $A_{950}$ at 950$cm^{-1}$ ($Q^2$) to that of $A_{1100}$ at 1100 $cm^{-1}$ ($Q^3$) as follows:

$$\frac{[Q^2]}{[Q^3]} = \alpha \frac{A_{950}}{A_{1100}} \tag{2}$$

$$2[Q^2] + 3[Q^3] + 4[Q^4] = X \tag{3}$$

$$[Q^2] + [Q^3] + [Q^4] = 1 \tag{4}$$

The correlation factor $\alpha$ contains the Raman scattering cross-sections at 950 and 1100 $cm^{-1}$ bands. $X$ is the average number of bridging oxygens per silicon atom. Since $X = 3$ for the compositions of (33-$x$)$Na_2O$-$x$RO-67$SiO_2$, the relation of $[Q^2] = [Q^4]$ is derived from the equations (3) and (4). The equilibrium constant $K$ for the reaction (1) is derived as the following equation.

$$\ln K = \ln \frac{[Q^2][Q^4]}{[Q^3]^2} = \ln \frac{[Q^2]^2}{[Q^3]^2} = \ln \left( \frac{A_{950}}{A_{1100}} \right)^2 + \ln \alpha \tag{5}$$

## 3. Results and Discussion

### 3.1 Raman spectra and their band deconvolution

Typical examples of polarized Raman spectra (25ºC HH and VH) and high-temperature spectra (700-1500ºC) of 8$Na_2O$-25CaO-67$SiO_2$ are summarized in Fig.2 (a). All the spectra were corrected using Bose-Einstein factor and normalized as the maximum of the 1100$cm^{-1}$ peak is unity. The bands near 600$cm^{-1}$ are assigned to the bending vibration associated with Si-O-Si linkages [10]. The bands at 950 and 1100$cm^{-1}$ have been assigned to the symmetric Si-$O^-$ stretching vibrations of $Q^2$ and $Q^3$ units, respectively [7,10]. The notable feature of the high-temperature spectra was that the relative intensity of the 950$cm^{-1}$ band to the 1100$cm^{-1}$ band seemed to increase with increasing temperature. Comparing 25ºC-HH and VH polarized spectra, the 1100$cm^{-1}$ band of VH spectrum shows larger FWHM than that of HH spectrum, showing that another band elements are considered to deconvolute the bands in the high-frequency region.

Figure 2 (b) shows the deconvolution of the high-frequency bands of 25ºC-HH, VH polarized spectra and the high-temperature spectrum (1300ºC) of 8$Na_2O$-25CaO-67$SiO_2$. Both 25ºC-HH and VH polarized spectra were well fitted (correlation factor: R>0.997) with four Gaussian-shaped elements having peaks near 950, 1050, 1100 and 1170$cm^{-1}$. The bands near 950 and 1100$cm^{-1}$ correspond to the Si-$O^-$ stretching vibrations of $Q^2$ and $Q^3$, respectively. The bands near 1050 and 1170$cm^{-1}$ are attributed to the Si-$O^0$ from bridging oxygen [7]. High-temperature Raman spectra were also well fitted with four Gaussian-shaped bands. As in Fig.2 (b), the $A_{950}/A_{1100}$ of 1300ºC was apparently larger than that of 25ºC-HH, showing that the molar fraction of $[Q^2]/[Q^3]$ increases with increasing temperature.

All the high-temperature Raman spectra of (33-$x$)$Na_2O$-$x$RO-67$SiO_2$ (R=Mg, Ca, Ba; $x$=0, 8, 17, 25) were deconvoluted taking into account the peak position and FWHM obtained from HH and VH polarized spectra of the corresponding glasses. Temperature dependences of the equilibrium constant $K$ were estimated from the $A_{950}/A_{1100}$ at various temperatures for each composition.

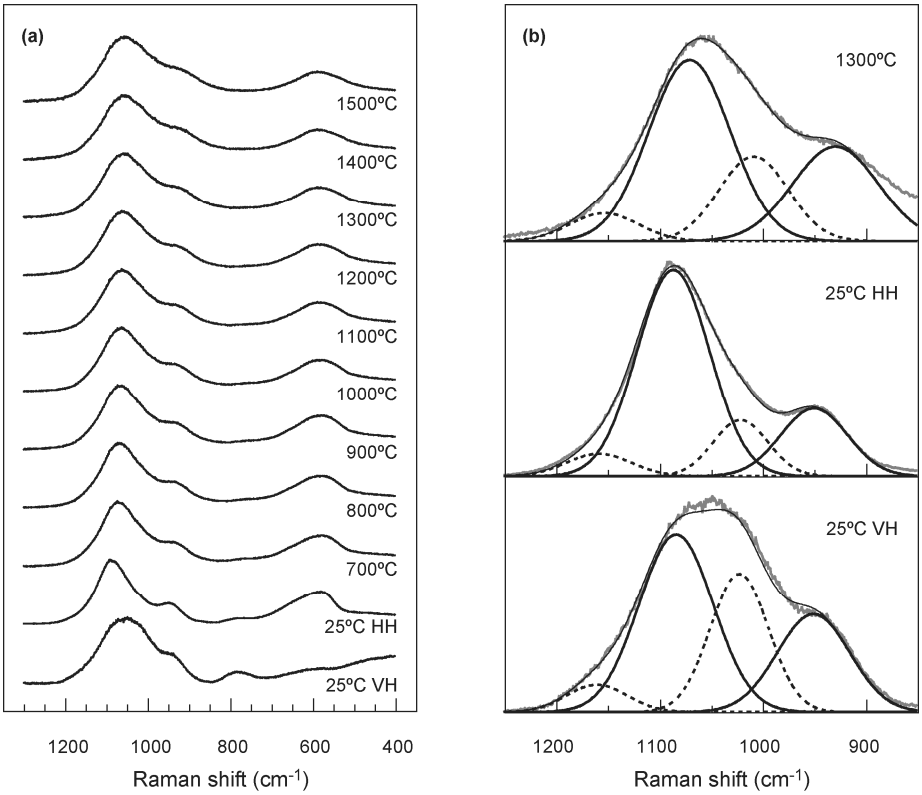


Fig. 2 (a) 25ºC-HH VH polarized Raman spectra and high-temperature Raman spectra (700-1500ºC). (b) An example of deconvolution of Raman spectra of $8Na_2O$-25CaO-$67SiO_2$ glass and melt.

### 3.2 Temperature dependence of the equilibrium constant *K*

In order to estimate the equilibrium constant $K$ for the reaction (1) from the $A_{950}/A_{1100}$, the reliable examination of $\alpha$ in Eq. (5) for each composition is necessary. Practically, $\alpha$ can be determined by the comparing the $A_{950}/A_{1100}$ with the $[Q^2]/[Q^3]$ ratio derived from $^{29}$Si MAS-NMR spectrum [14]. However the NMR data, which appropriate for compositions of $(33\text{-}x)Na_2O$-$xRO$-$67SiO_2$ have not been reported. We alternatively used $K_R$, which is given by the following equation, instead of $K$.

$$\ln K_R = \ln K - \ln \alpha = \ln\left(\frac{A_{950}}{A_{1100}}\right)^2 \tag{6}$$

Shown in Fig. 3 are the plots of $\ln K_R$ vs. $1/T$ where the $A_{950}/A_{1100}$ were used to obtain $K_R$ from Eq. (6). In the figure, plots at temperatures above the glass transition are fitted with a linear function by the least squares. Temperature dependences of $\ln K_R$ reflect the framework structures from high temperature to room temperature.

In the case of R=Mg and Ca, plots of $\ln K_R$ at 1500ºC were high irrespective of $x$; large amounts of $Q^2$ and $Q^4$ units are formed in the melts. However, temperature dependences of $\ln K_R$ show the clear difference between $0 \le x \le 17$ and $x=25$. Temperature dependences of $\ln K_R$ in the compositional range of $0 \le x \le 17$ ($[RO] \le [Na_2O]$) are less sensitive to $x$. In $x>17$ ($[RO]>[Na_2O]$), however, temperature dependences of $\ln K_R$ drastically change with the mixing ratio of RO to $Na_2O$. Consequently, the framework structure of resultant glass is considered to depend strongly on $x$ in the compositional range of $x>17$ ($[RO]>[Na_2O]$). Interestingly, the mixing ratio of CaO to $Na_2O$ of the commercial soda-lime glass is about 0.8, and in the region of $[CaO]<[Na_2O]$. This means that $Q^n$ distributions, which structured framework, would not be affected by the compositional fluctuation. Their melt properties would also be stable, result in the stable glass production.

On the other hand, temperature dependences of $\ln K_R$ for R=Ba is less sensitive in the whole compositional range of $0<x \le 25$, showing that the framework structures are similar irrespective of the mixing ratio of BaO to $Na_2O$ from the viewpoint of $Q^n$ distribution.

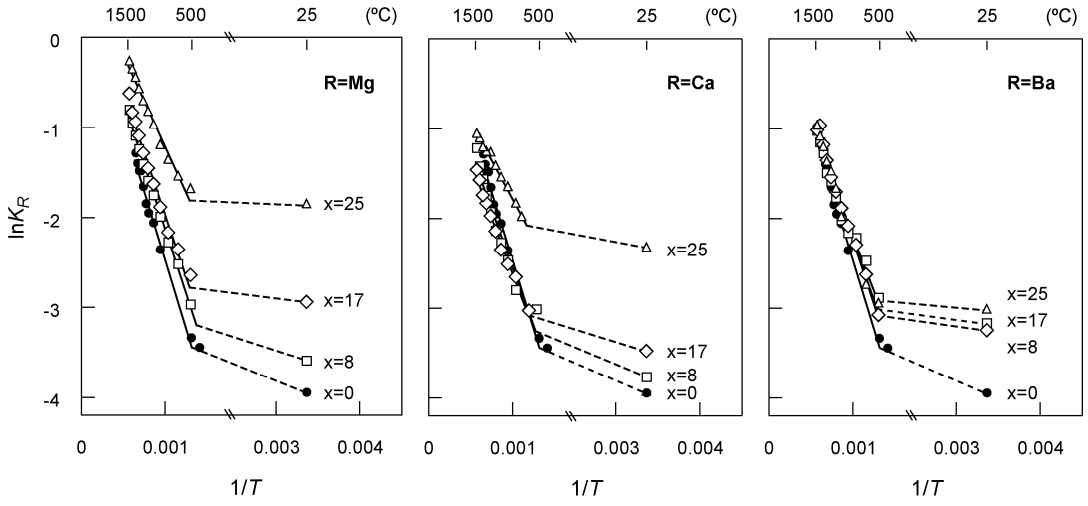


Fig.3 Plots of $\ln K_R$ vs. 1/T for (33-$x$)$Na_2O$-$x$RO-67$SiO_2$ (R=Mg, Ca, Ba; $x$=0, 8, 17, 25).

**3.3 Effects of mixing of alkali and alkaline-earth on the framework structure of glass and melt**

Changes of framework structure under the cooling process are closely related to the $Q^n$ equilibration, which is generally expressed as the equilibrium reaction (1). Assuming that $\alpha$ is independent of temperature, the enthalpy change $\Delta H$ for the reaction (1) is given by the slope of $\ln K_R$ vs. $1/T$ in Fig. 3 using the following equation,

$$\frac{-\Delta H}{R} = \frac{\partial(\ln K)}{\partial(1/T)} \approx \frac{\partial\left(\ln K_R\right)}{\partial(1/T)}. \tag{7}$$

Compositional dependences of $\Delta H$ for (33-$x$)$Na_2O$-$x$RO-67$SiO_2$ (R=Mg, Ca, Ba) are shown in Fig. 4, in which the effects of mixing of $Na_2O$ and RO on the $Q^n$ equilibrium are clearly found. As RO substitutes for $Na_2O$, $\Delta H$ decreases with increasing $x$. In R=Mg and Ca, $\Delta H$ at $x \leq 17$ decreases gradually with increasing $x$, whereas, at $x>17$ it steeply decreases. On the other hand, in the melts of R=Ba, $\Delta H$ show a steady decrease with increasing $x$ even at x>17. The inflections of $\Delta H$ in Fig. 4 indicate that the modifying cation governing the $Q^n$ equilibrium is surely switched from sodium to alkaline-earth ion with increasing $x$.

The simplest expressions of the disproportionation reaction for binary alkali silicate melts and binary alkaline-earth silicate melts are described as the reaction (1). However, when we take the counter cation of an NBO in $Q^n$ into account, the elementary reaction of alkaline-earth silicate melt (e.g. R=Ca) can be described as follow,

$$2Q^3_{(Ca)} \Leftrightarrow Q^2_{(Ca)} + Q^4, \tag{8}$$

where $Q^3_{(Ca)}$ means that one NBO in the $SiO_4$ tetrahedron interacts with one $Ca^{2+}$ ion, and $Q^2_{(Ca)}$ means two NBOs in the tetrahedron interact with one $Ca^{2+}$ ion. On the other hand, another type of $Q^2$ can be considered; $Q^2_{(Ca,Ca)}$ which interacts with two $Ca^{2+}$ ions via two NBOs in the tetrahedron. In this case, the reaction (8) has to be corrected as follow,

$$4Q^3_{(Ca)} \Leftrightarrow 2Q^2_{(Ca,Ca)} + 2Q^4, \tag{9}$$

where the twice number of tetrahedra is required to cause the disproportionation reaction. This reaction has to be distinguished from the reaction (1) and (8), and would affect $Q^n$ distributions in the melts containing large amount of RO. From the viewpoint of the configuration of $SiO_4$ tetrahedron and bivalent cation, the reaction (9) would be more plausible than the reaction (8). Therefore, in the melt containing large amount of alkaline-earth oxide ([RO]>[$Na_2O$]), the reaction (9) is considered to dominate the disproportionation reaction.

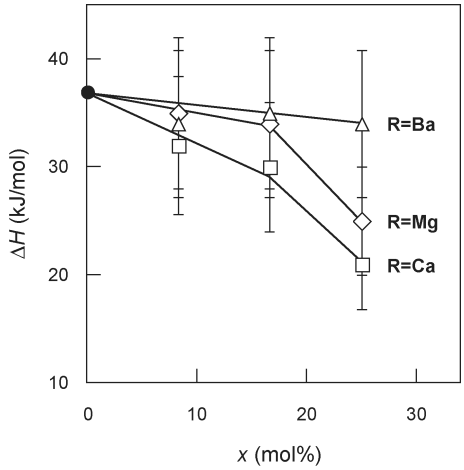


Fig.4 Compositional dependences of $\Delta H$ for (33-$x$)$Na_2O$-$x$RO-67$SiO_2$ (R=Mg, Ca, Ba; $x$=0, 8, 17, 25).

## 4. Conclusion

High-temperature Raman spectra of (33-$x$)$Na_2O$-$x$RO-67$SiO_2$ glass melts (R=Mg, Ca, Ba; $x$=0-25) were measured at various temperatures from 1500ºC to room temperature. The equilibrium constants $K_R$ and the enthalpy change $\Delta H$ for the reaction $2Q^3 \Leftrightarrow Q^2 + Q^4$ in the melts were estimated by the band deconvolution of the spectra. In R=Mg and Ca, $\Delta H$ at $x \leq 17$ decreases gradually with increasing $x$, whereas, at $x>17$ it steeply decreases. On the other hand, in the melts of R=Ba, $\Delta H$ show a steady decrease with increasing $x$ even at x>17. These results suggest that the modifying cation governing the $Q^n$ equilibrium is surely switched from sodium to alkaline-earth ion with increasing $x$. The compositional dependences are considered to be due to the difference in the elementary reaction of the $Q^n$ equilibrium between alkali silicate melts and alkaline-earth silicate melts. Further research on the determination of the $Q^n$ distributions for (33-$x$)$Na_2O$-$x$RO-67$SiO_2$ glasses by using $^{29}$Si MAS-NMR spectroscopy would give an authenticity of the effects of mixing of $Na_2O$ and RO on both the $Q^n$ equilibrium in the melts and the framework structure of the resultant glasses.

## 5. References


[1] J.F. Stebbins, *J. Non-Cryst. Solids*, **106**, 359-369 (1988).
[2] H. Maekawa, T. Maekawa, K. Kawamura and T. Yokokawa, *J. Non-Cryst. Solids*, **127**, 53-64 (1991).
[3] S. Shimokawa, H. Maekawa, E. Yamada, T. Maekawa, Y. Nakamura and T. Yokokawa, *Chem. Lett.*, 617-620 (1990).
[4] J.F. Stebbins, I. Farnan and X. Xue, *Chem. Geol.*, **96**, 371-385 (1992).
[5] F.A. Seifert, B.O. Mysen and D. Virgo, *Geochim. Cosmochim. Acta*, **45**, 1879-1884 (1981).
[6] B.O. Mysen and J.D. Frantz, *Chem. Geol.*, **96**, 321-332 (1992).
[7] B.O. Mysen and J.D. Frantz, *Contrib. Mineral Petrol.*, **117**, 1-14 (1994).
[8] P.F. McMillan, *Am. Mineral.*, **69**, 622-644 (1984).
[9] P.F. McMillan, G.H. Wolf and B.T. Poe, *Chem. Geol.*, **96**, 351-366 (1992).
[10] P.F. McMillan, "Vibrational spectroscopy of silicate liquids"; pp.247-315 in *Structure, dynamics, and properties of silicate melts*, Edited by J.F. Stebbins, P.F. McMillan and D.B. Dingwell, Mineralogical Society of America, Washington D.C., 1995.
[11] T. Yano, N. Kunimine, E. Matsuki, S. Shibata and M. Yamane, *Proceedings of Fundamentals of glass science and technology*, Växjö, 8-14 (1997).
[12] T. Yano, T. Kobayashi, S. Shibata and M. Yamane, *Phys. Chem. Glass*, **43C**, 90-95 (2002).
[13] T. Yano, N. Kunimine, S. Shibata and M. Yamane, *J. Non-Cryst. Solids*, **321**, 137-146, 147-156, 157-168 (2003).
[14] T. Maehara, T. Yano, S. Shibata and M. Yamane, *Philos. Mag.*, accepted.
[15] D.W. Marquardt, *J. Soc. Ind. Appl. Math.*, **11**, 431-441 (1963).